CHALMERS
UNIVERSITY OF TECHNOLOGY

Kinetics and Efficiency of Triplet-Triplet Annihilation Photon Upconversion under Pulsed Excitation Conditions

Kinetics and Efficiency of Triplet-Triplet Annihilation Photon Upconversion under Pulsed Excitation Conditions

Chen Ye,[a] Bo Albinsson,*[b] and Karl Börjesson*[a]

Triplet-triplet annihilation is a promising method to convert low energy photons to high energy ones. Due to the long timescales and the bimolecular nature of the process, the overall efficiency of triplet-triplet annihilation greatly depends on the excitation type and intensity. Upconversion efficiencies are usually measured using continuous wave conditions. Here we develop an analytical and experimental method to investigate how the excitation modulation affects the triplet-triplet annihilation efficiency. The simulated and experimental results demonstrate high consistency. The triplet-triplet annihilation efficiency drops as expected with increasing excitation frequency at a fixed average power density, which our simulations accurately predicts. The method described here allows to relate efficiencies measured at pulsed conditions with those measured at continuous wave conditions.

Triplet-triplet annihilation photon-upconversion (TTA-UC) provides the possibility of converting low-energy to high-energy photons, and is thus a promising method to promote solar energy harvesting.[1] The phenomenon was discovered by Hatchard and Parker in the 1960s, and involves the close interaction between two triplet excited annihilators (Scheme 1a).[2] In this exothermic process one of the triplet annihilators is relaxed to the ground state, while the other is excited to the first excited singlet state from where a photon can be emitted.[3] TTA is a special example of Dexter energy transfer, and requires a short interaction range (typically <10 Å).[4] However, due to diffusion outcompeting triplet relaxation, TTA can be efficient at non-coherent conditions. Furthermore, unlike second-harmonic generation and two-photon absorption, TTA-UC shows considerable efficiency even at low photon flux. This advantage makes TTA-UC a promising method for applications where solar and even sub-solar conditions are required. Recently, TTA-UC has been successfully incorporated into solar cells,[5] photocatalysis,[6] optical devices,[7] as to increase solar energy utilization. The fast development of TTA-UC requires continuous and fundamental research on both system design and mechanisms. The upconversion efficiency and threshold excitation energy are two main figures of merits for TTA-UC. It is therefore important to be able to compare these figures of merits between different experimental conditions. Pioneering studies pointed out that with increasing excitation intensity, the TTA efficiency changes from a quadratic to a linear dependency on the excitation intensity.[8]

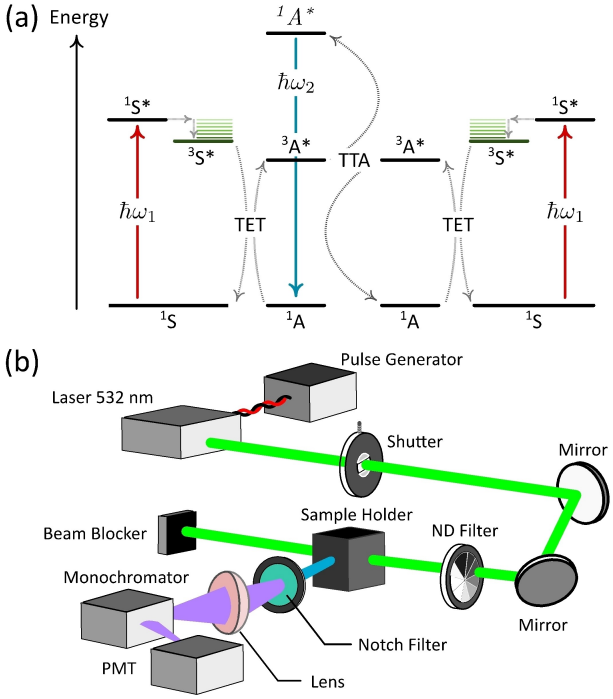

Scheme 1. (a) Schematic illustration of the TTA process. (b) Experimental setup of TTA-UC under pulsed excitation.

In this work, we derived a theoretical expression that relates the TTA-UC efficiency with the mode of excitation. We used a modulated laser to illuminate a benchmark TTA-UC combination in solution and measure the relationship between TTA-UC efficiency and the excitation type (Scheme 1b). The TTA-UC efficiency drops, as expected, with the excitation frequency under a constant excitation power density, a drop that is here quantitatively simulated. Thus, the result provides experimental and analytical methods for analyzing the non-linear photo-

[a] *Dr. C. Ye, Dr. K. Börjesson*
Department of Chemistry and Molecular Biology
University of Gothenburg
Gothenburg, Sweden.
E-mail: karl.borjesson@gu.se
[b] *Prof. B. Albinsson*
Department of Chemistry and Chemical Engineering,
Chalmers University of Technology
Gothenburg, Sweden
E-mail: balb@chalmers.se

Supporting information for this article is available on the WWW under https://doi.org/10.1002/cmtd.202000046

chemical process of TTA-UC under different types of excitation conditions.

Here we use 9,10-diphenylanthracene (DPA) as annihilator, due to its high quantum yields of both fluorescence and TTA (SI 1).[9] Annihilators in their first excited triplet state were generated by triplet-triplet energy transfer (TTET) from a triplet sensitizer (platinum octaethylporphyrin, PtOEP). After the initial excitation to the first excited state of PtOEP, energy is rapidly relaxed via intersystem crossing to the first excited triplet state. PtOEP in this long-lived state collide with DPA and the energy is transferred via TTET. Then two annihilators in their first excited triplet state collide, and undergo TTA. The kinetics of TTA can be described with the following ordinary differential equation (eq.1):[10]

$$\frac{d\rho}{dt} = G(t) - 2k_{TTA}\rho^2 - k_T\rho \quad (1)$$

where ρ is the concentration of triplet annihilators, t is the time after excitation, k_{TTA} is the second order TTA rate constant, and k_T is the pseudo first order (including the monomolecular decay and the bimolecular decay with oxygen) intrinsic rate constant of triplet annihilators. G is a time dependent generation function of triplet annihilators, which contain sensitizer excitation and TTET to annihilators. These kinetic parameters can be determined from transient absorption spectroscopy. The T_1 to T_n transition of DPA induces an excited state absorption signal at 410 nm, which is much longer-lived than the ground state bleaching signal of PtOEP (Figure 1a). The kinetics of triplet DPA can therefore be monitored by the decay of the excited state absorption signal at long time ranges

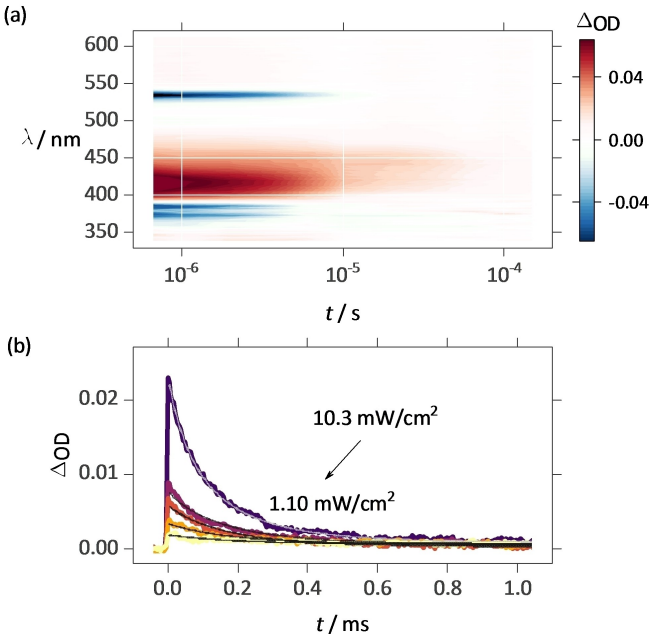

Figure 1. (a) Transient absorption map of 4 μM PtOEP and 100 μM DPA in toluene after excitation at 537 nm (6.20 mW/cm^2, 10 Hz). (b) Excited state absorption decay and the corresponding global fit at 410 nm after excitation at 537 nm with different power densities (4 μM PtOEP and 1 mM DPA).

(Figure 1b). Nanosecond transient absorption spectroscopy uses a Nd:YAG laser as excitation source and thus provides intensive (~1 mJ per pulse) and short (around 10 ns) pulses. TTET from the sensitizer to the annihilator is diffusion controlled, and considering the large diffusion rate constants and high concentration of the ground state annihilator, TTET can be fast and efficient.[11] We can consequently consider the formation of triplet annihilators as quasi-instant upon excitation. The initial condition of eq. 1 is therefore:

$$\rho|_{t=0} = \frac{\alpha I_{ex}}{f} \quad (2)$$

where α is a pre-factor for triplet generation, I_{ex} is the excitation power density, and f is the excitation frequency. The energy input by a single pulse equals to I_{ex}/f. The linear dependence of the initial condition on the excitation intensity is based on the pre-assumptions of an instant excitation and fast energy transfer, and the pre-factor α encompasses the probabilities of both excitation and energy transfer. By varying the excitation intensity, we calculated the TTA kinetic parameters by global fitting of eqs. 1 and 2 to the long time (>1 μs) decay (Table 1 and Figure 1b).[12]

The calculated kinetic parameters are used to simulate the dynamics and the steady-state behavior of TTA-UC when the excitation source is running at a frequency f with an average power density, I_{ex}.[14] Due to the linear relationship between triplet generation and the average excitation powder density, the triplet generation remains constant when the frequency is changed. However, the peak intensity of a single pulse drops with increasing excitation frequency at a constant average power, and it will affect the TTA kinetics and efficiency. With an ideal excitation pulse (i.e. a Dirac pulse), the TTA kinetics can be treated as an array of ordinary differential equations with periodic number i (eq. 3):

$$\begin{cases} \frac{d\rho[i]}{dt} = -2k_{TTA}\rho[i]^2 - k_T\rho[i] \\ \rho[i]|_{t=0} = \rho[i-1]|_{t=1/f} + \frac{\alpha I_{ex}}{f} \end{cases} \quad (3)$$

where a period is defined as the time window between the starting points of two adjacent pulses, ρ[i] is the time dependent density concentration of triplet annihilators in period i, and t is the time after the beginning of the corresponding period. When the excitation frequency is low, the triplet annihilators decay completely before the next excitation pulse occurs (independent periods). All the TTA periods are then independent. However, when the excitation frequency increases, the

Table 1. TTA kinetic parameters of DPA in toluene.

$\varepsilon(T_1-T_n)$/cm^{-1}M^{-1} [a]	k_{TTA}/M^{-1}s^{-1}	k_T/s^{-1}	α/M cm^2 mJ^{-1} [b]
15600	$2.6\pm0.1\times10^9$	$4.7\pm0.1\times10^3$	$1.4\pm0.0\times10^{-6}$

[a] Molar absorptivity of the excited state absorption peak of triplet DPA at 410 nm in deoxygenated toluene.[13] [b] The value of the pre-factor is for a 1 cm light path length cuvettes with 4 μM PtOEP and 1 mM DPA.

triplet decay time is longer than the period duration (Figure 2). The concentration of triplet annihilators is non-zero at the end of the period, and therefore affects the next period (correlated periods). When the excitation frequency approaches infinite, the TTA system can be approximated with a continues-wave excitation mode (CW mode). Using the kinetic parameters from Table 1, the TTA kinetics was simulated at a constant average power but different excitation frequencies (Figure 2)

As seen in Figure 2, the systems can reach an equilibrium state, where the kinetics is periodical number independent for both correlated and independent periods. Eq. 3 can be analytically solved, leading to the following expression (SI 2):

$$\rho_0 = \frac{\rho_0 e^{-k_T/f}}{1 + \frac{2k_{TTA}\rho_0}{k_T}(1 - e^{-k_T/f})} + \frac{\alpha I_{ex}}{f} \tag{4}$$

where ρ_0 is triplet annihilator concentration at the beginning of every period when equilibrium has occurred. Since I_{ex} and f are experimental parameters, eq. 4 reduces to a quadratic equation in ρ_0, with one positive root. At high excitation frequencies, triplet annihilators do not decay completely within a single period. Triplet decay is intervened by the next pulse, and the triplet annihilators will accumulate with periods. When the initial concentration of triplet annihilator reaches the constant ρ_0, the TTA efficiency over time also becomes a constant. The average TTA-UC intensity of the repeated excitation system at the equilibrium state can be described by eq. 5:

$$\begin{cases} I_{TTA} = f\int_0^{1/f} k_{TTA}\rho^2 dt \\ \rho|_{t=0} = \rho_0 \end{cases} \tag{5}$$

For a TTA system under repeated excitation, the system will reach the steady-state condition after an initial buildup of the concentration of triplet annihilators (Figure 2). At this stage, the average TTA-UC intensity of the system can be approximated by the TTA-UC intensity at the equilibrium state. We solved eq. 4 and eq. 5 over wide ranges of both excitation power densities and excitation frequencies, and then simulated the steady state TTA behavior under these conditions (Figure 3). When the average excitation power density is constant, the energy input into the TTA system is also a fixed value. However, the TTA-UC intensity changes with the excitation frequency. At the low frequency region, the TTA-UC intensity drops dramatically with increasing excitation frequency. This is because the density of triplet annihilators decreases and the probability of monomolecular decay increases (Eq. 3). Further increasing the excitation frequency leads to the intervening of triplet decay kinetics over excitation periods. At this stage, the TTA efficiency as a function of excitation frequency reaches a constant value, which corresponds to the TTA efficiency under continuous wave excitation.[15]

The simulation describes the relationship between TTA-UC efficiency and excitation type using an ideal pulse. Unlike the ideal pulse, the real pulses generated by a modulated laser last for a certain time window. To take the pulse width into account, the triplet annihilators generated by the pulse in the initial conditions of eq. 3 is replaced with a generation factor G(t),

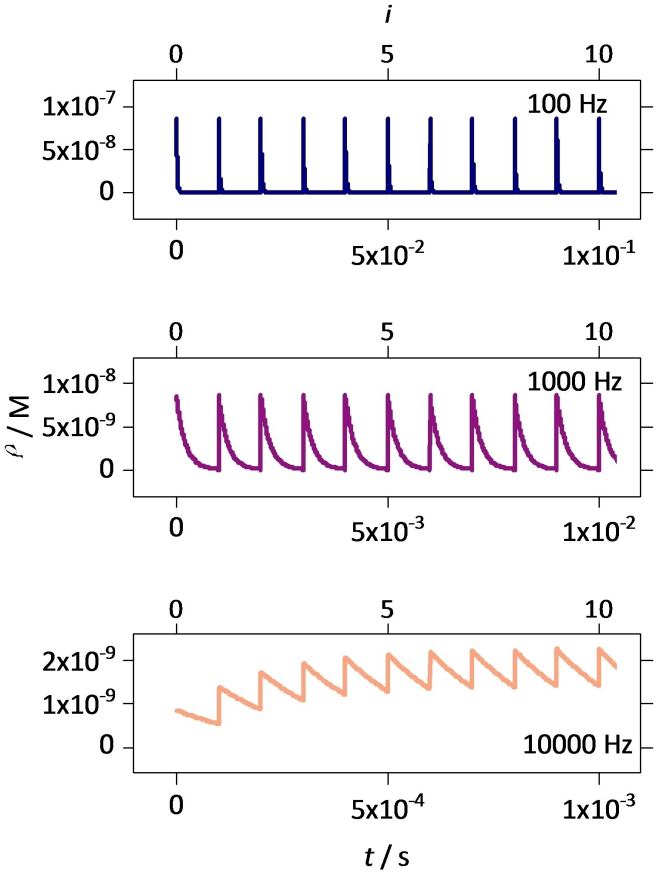

Figure 2. Simulated concentration of triplet DPA as a function of time at different excitation frequencies. The simulation is based on 4 μM PtOEP and 1 mM DPA in a 1 cm×1 cm cuvette and a constant average excitation power density of 6 mW/cm^2.

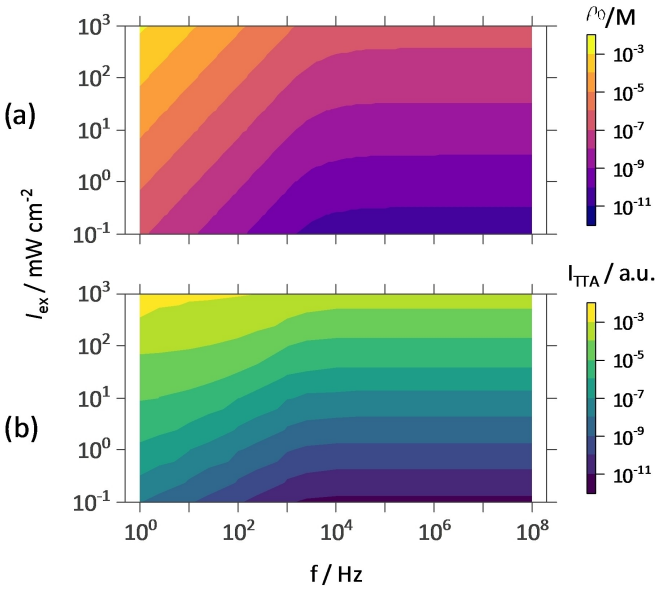

Figure 3. Simulated TTA-UC parameters of DPA in toluene as functions of excitation power density and excitation frequency: (a) initial triplet concentration at the equilibrium state, ρ_0. (b) average TTA-UC intensity, I_{TTA}.

which have the shape of the measured laser pulse. For a short pulse, the triplet generation can be considered as fast and instant. However, simulations show a negative correlation between the TTA efficiency and the pulse duration when the pulse length approaches the lifetime of triplet annihilators (Figure S1). When the pulse duration is comparable to the triplet decay time window, the TTA kinetics behave like the CW model.

To support the theoretical analysis, we used a home-made TTA-UC setup to test the TTA behaviour of PtOEP and DPA in toluene solution under pulsed excitation conditions. A modulated CW laser coupled to a pulse generator was used to provide the pulsed excitation and a graded neutral density filter (ND filter) was used to tune the excitation intensity to keep the average power density constant (Scheme 1, SI 3). The TTA-UC emission was passed through a monochromator and detected by a photomultiplier tube (PMT). A notch filter was used to remove scattered laser light. PtOEP was excited at 532 nm, and the upconverted fluorescence from DPA was observed at 430 nm, providing a 0.55 eV anti-Stokes shifted emission (Figure 4a). The phosphorescence from the sensitizer at 650 nm was strongly quenched, indicating an efficient and fast TTET from sensitizer to annihilator. The pulse shape was recorded by a PMT connected to an oscilloscope. The shape of the pulse provided the time dependent function of triplet annihilator generation under real excitation conditions ($G(t)$, Figure S2). We finally set the average excitation power density to 6 mW/cm^2 with a fixed pulse width of 20 µs. As shown in Figure 4b, the TTA intensity drops continuously with increasing excitation frequency from 50 Hz to 2000 Hz, and approaches a constant value when the frequency is higher than 2000 Hz. Since the average power density is constant, the TTA efficiency is excitation frequency dependent. The experimental data follows the simulated relationship for both an ideal pulse model and the real pulse model (Figure 4b), without systematic deviations between theory and experiment (Figure 4c). The high consistency between experimental and simulated results show that the TTA efficiency as a function of excitation type can be well descried within a model of periodical excitation. The TTA-UC quantum yields were further calculated with cresyl violet in methanol solution as the reference (Figure S4). The calculated TTA-UC quantum yields are close to the simulated values, showing the practical validity of the methodology.

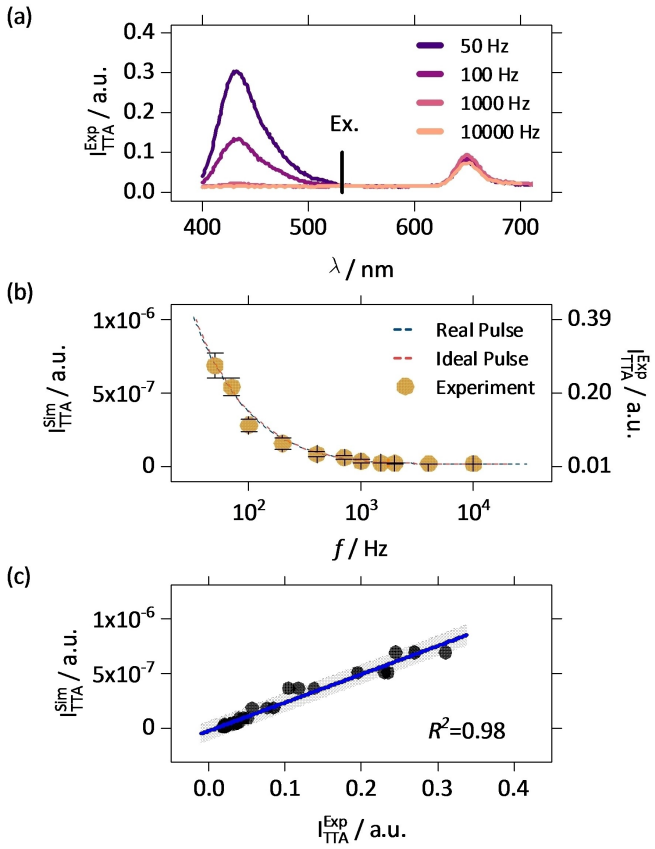

Figure 4. (a) Photon upconversion emission spectra of a sample containing 4 µM PtOEP and 1 mM DPA in toluene under different excitation frequencies, but with a constant power density of 6 mW/cm^2; (b) Simulated TTA reaction intensity and the experimental data; (c) Correlation between simulated data (real pulse) and the experimental data.

In conclusion, we here present a method to simulate the relationship between TTA efficiency and excitation modulation. Kinetic parameters were obtained from transient absorption spectroscopy, and the numerical simulations were achieved by dividing the periodic kinetic function into a kinetic array involving only a single pulse. Experimental results from a home-made setup with a modulated laser as excitation source showed excellent agreement with simulations. The triplet-triplet annihilation efficiency drops as expected with increasing excitation frequency, which our simulations accurately predicts. The method described here allows the relation between efficiencies measured at pulsed conditions with those measured at continuous wave conditions, which needs high excitation power density for a detectable signal.

Acknowledgements

We gratefully acknowledge financial support from the European Research Council (ERC-2017-StG-757733), the Swedish Energy Agency (36436-2) and the Knut and Alice Wallenberg Foundation (KAW 2017.0192).

Conflict of Interest

The authors declare no conflict of interest.

Keywords: Kinetics · Pulsed Excitation · Simulation · Triplet-triplet annihilation

[1] T. F. Schulze, T. W. Schmidt, *Energy Environ. Sci.* **2015**, *8*, 103–125.
[2] a) N. Yanai, N. Kimizuka, *Acc. Chem. Res.* **2017**, *50*, 2487–2495; b) V. Gray, K. Moth-Poulsen, B. Albinsson, M. Abrahamsson, *Coord. Chem. Rev.* **2018**, *362*, 54–71.
[3] a) A. Monguzzi, J. Mezyk, F. Scotognella, R. Tubino, F. Meinardi, *Phys. Rev. B* **2008**, *78*; b) T. W. Schmidt, F. N. Castellano, *J. Phys. Chem. Lett.* **2014**, *5*, 4062–72.

[4] A. Monguzzi, R. Tubino, F. Meinardi, *Phys. Rev. B* **2008**, *77*.
[5] a) S. P. Hill, K. Hanson, *J. Am. Chem. Soc.* **2017**, *139*, 10988–10991; b) T. Dilbeck, K. Hanson, *J. Phys. Chem. Lett.* **2018**, *9*, 5810–5821.
[6] a) K. Börjesson, D. Dzebo, B. Albinsson, K. Moth-Poulsen, *J. Mater. Chem. A* **2013**, *1*, 8521–8524; b) C. Kerzig, O. S. Wenger, *Chem. Sci.* **2018**, *9*, 6670–6678; c) B. D. Ravetz, A. B. Pun, E. M. Churchill, D. N. Congreve, T. Rovis, L. M. Campos, *Nature* **2019**, *565*, 343–346; d) B. Pfund, D. M. Steffen, M. R. Schreier, M.-S. Bertrams, C. Ye, K. Börjesson, O. S. Wenger, C. Kerzig, *J. Am. Chem. Soc.* **2020**, *142*, 10468–10476.
[7] a) K. Börjesson, P. Rudquist, V. Gray, K. Moth-Poulsen, *Nat. Commun.* **2016**, *7*, 12689; b) C.-H. Chen, N. T. Tierce, M.-k. Leung, T.-L. Chiu, C.-F. Lin, C. J. Bardeen, J.-H. Lee, *Adv. Mater.* **2018**, *30*, 1804850; c) D. Yang, J. Han, M. Liu, P. Duan, *Adv. Mater.* **2018**, *31*, 1805683; d) D. Polak, R. Jayaprakash, T. P. Lyons, L. Á. Martínez-Martínez, A. Leventis, K. J. Fallon, H. Coulthard, D. G. Bossanyi, K. Georgiou, I. I. A. J. Petty, J. Anthony, H. Bronstein, J. Yuen-Zhou, A. I. Tartakovskii, J. Clark, A. J. Musser, *Chem. Sci.* **2020**, *11*, 343–354; e) C. Ye, S. Mallick, M. Kowalewski, K. Börjesson, *ChemRxiv. Preprint.* **2020**, 10.26434/chemrxiv.12806861.v1.
[8] a) A. Monguzzi, J. Mezyk, F. Scotognella, R. Tubino, F. Meinardi, *Phys. Rev. B* **2008**, *78*, 195112; b) A. Haefele, J. Blumhoff, R. S. Khnayzer, F. N. Castellano, *J. Phys. Chem. Lett.* **2012**, *3*, 299–303.
[9] a) V. Gray, D. Dzebo, M. Abrahamsson, B. Albinsson, K. Moth-Poulsen, *Phys. Chem. Chem. Phys.* **2014**, *16*, 10345–52; b) V. Gray, K. Börjesson, D. Dzebo, M. Abrahamsson, B. Albinsson, K. Moth-Poulsen, *J. Phys. Chem. C* **2016**, *120*, 19018–19026.
[10] a) C. Ye, V. Gray, J. Mårtensson, K. Börjesson, *J. Am. Chem. Soc.* **2019**, *141*, 9578–9584; b) C. Ye, V. Gray, K. Kushwaha, S. Kumar Singh, P. Erhart, K. Börjesson, *Phys. Chem. Chem. Phys.* **2020**, *22*, 1715–1720.
[11] Q. Chen, Y. Liu, X. Guo, J. Peng, S. Garakyaraghi, C. M. Papa, F. N. Castellano, D. Zhao, Y. Ma, *J. Phys. Chem. A* **2018**, *122*, 6673–6682.
[12] T. N. Singh-Rachford, F. N. Castellano, *Coord. Chem. Rev.* **2010**, *254*, 2560–2573.
[13] I. Carmichael, W. P. Helman, G. L. Hug, *J. Phys. Chem. Ref. Data* **1987**, *16*, 239–260.
[14] J. Partee, E. L. Frankevich, B. Uhlhorn, J. Shinar, Y. Ding, T. J. Barton, *Phys. Rev. Lett.* **1999**, *82*, 3673–3676.
[15] F. Deng, J. Blumhoff, F. N. Castellano, *J. Phys. Chem. A* **2013**, *117*, 4412–4419.

Manuscript received: September 7, 2020
Version of record online: November 18, 2020